Feasibility of packed-bed trickling filters for partial nitritation/anammox : effects of carrier material, bottom ventilation openings, hydraulic loading rate and free ammonia

Feasibility of packed-bed trickling filters for partial nitritation/anammox: Effects of carrier material, bottom ventilation openings, hydraulic loading rate and free ammonia

Yankai Xie [a, b], Mingsheng Jia [c], Fabian De Wilde [c], Katrien Daeninck [c], Haydée De Clippeleir [c], Willy Verstraete [c, d], Siegfried E. Vlaeminck [a, *]

[a.] Research Group of Sustainable Energy, Air and Water Technology (DuEL), Department of Bioscience Engineering, University of Antwerp, Groenenborgerlaan 171, 2020 Antwerpen, Belgium

[b.] State Key Joint Laboratory of Environment Simulation and Pollution Control, School of Environment, Tsinghua University, Beijing 100084, China

[c.] Center for Microbial Ecology and Technology (CMET), Ghent University, Coupure Links 653, 9000 Gent, Belgium

[d.] Avecom NV, Industrieweg 122P, 9032 Wondelgem, Belgium

* Corresponding author; E-mail: Siegfried.Vlaeminck@UAntwerpen.be

Abstract

This study pioneers the feasibility of cost-effective partial nitritation/anammox (PN/A) in packed-bed trickling filters (TFs). Three parallel TFs tested different carrier materials, the presence or absence of bottom ventilation openings, hydraulic loading rates (HLR, 0.4-2.2 $m^3\ m^{-2}\ h^{-1}$), and free ammonia (FA) levels on synthetic medium. The inexpensive Argex expanded clay was recommended due to the similar nitrogen removal rates as commercially used plastics. Top-only ventilation at an optimum HLR of 1.8 $m^3\ m^{-2}\ h^{-1}$ could remove approximately 60% of the total nitrogen load (i.e., 300 mg N $L^{-1}\ d^{-1}$, 30 °C) and achieve relatively low NO_3^--N accumulation (13%). Likely FA levels of around 1.3-3.2 mg N L^{-1} suppressed nitratation. Most of the total nitrogen removal took place in the upper third of the reactor, where anammox activity was highest. Provided further optimizations, the results demonstrated TF is suitable for low-energy shortcut nitrogen removal.

Keywords: anoxic ammonium-oxidizing bacteria; biological nitrogen removal; deammonification; nitrification; nitrite-oxidizing bacteria

1. Introduction

Minimizing resource and energy consumption, greenhouse gas emissions, and sludge production is critical for progress toward more sustainable wastewater treatment. Compared to conventional nitrification/denitrification, partial nitritation/anammox (PN/A) can save around 60% of the aeration energy, 100% of the organic carbon needs, and 90% of the sludge handling and transport costs for nitrogen removal from carbon-lean wastewaters (Mulder, 2003). In the PN/A process, about half of the ammonium (NH_4^+) is aerobically oxidized to nitrite (NO_2^-) by aerobic ammonium-oxidizing bacteria (AerAOB), and the residual NH_4^+ is oxidized with the produced NO_2^- to generate nitrogen gas (N_2) by anoxic ammonium-oxidizing or anammox bacteria, with the first biomass termed for AerAOB, and the second one for AnAOB (Vlaeminck et al., 2012). The overall PN/A stoichiometry is shown as Eq. (1).

$$NH_4^+ + 0.792\ O_2 + 0.080\ HCO_3^- \rightarrow 0.435\ N_2 + 0.111\ NO_3^- + 1.029\ H^+ + 0.052\ CH_{1.4}O_{0.4}N_{0.2} + 0.028\ CH_2O_{0.5}N_{0.15} + 1.460\ H_2O \quad (1)$$

Biofilm-based reactors are widely used for PN/A processes as they can retain the slow-growing AnAOB more easily than suspended growth systems such as sequencing batch reactors (SBR) containing suspended biomass (De Clippeleir et al., 2013; De Clippeleir et al., 2011; Vlaeminck et al., 2012). The lowered air supply by aeration pumps is considered a key factor to reduce wastewater treatment costs (Zekker et al., 2021a). As a type of passively aerated reactor, trickling filters (TFs) are packed-bed biofilm reactors with effluent flowing downwards and ambient oxygen diffusing into the biofilm, which have a low electricity demand for wastewater treatment (Séguret et al., 2000). In practice, TFs are often used as a post-treatment step of anaerobic sewage treatment for carbon oxidation and nitrification (Bressani-Ribeiro et al., 2021). In this case, TFs mainly allow for achieving high ammonium removal but not necessarily total nitrogen (TN) removal, especially in developing countries, e.g., Brazil and Ghana (Arthur et al., 2022; Bressani-Ribeiro et al., 2018; Bressani-Ribeiro et al., 2021; The Water Environment, 2011). Therefore, implementing PN/A in TFs may greatly expand their applications and offer a cost-effective alternative for TN removal. Besides, the high and steady temperatures in those tropical countries (between 20 °C and 35 °C all year long), could benefit the growth and activity of AerAOB and AnAOB (Lombard-Latune et al., 2018; Vlaeminck et al., 2012; Zekker et al., 2021b). Thus, the first application scenario of PN/A-TF is conceived in warm climates. To the knowledge of the authors, the only PN/A-TF reports used spongy polyurethane material as a compressible, non-conventional carrier material (Bressani-Ribeiro et al., 2021; Sánchez Guillén et al., 2015; Watari et al., 2020), whereas no tests results are available based on conventional non-compressible organic carriers (e.g. polypropylene, polyethylene) nor expanded clay as an inexpensive non-compressible mineral alternative.

The DO levels play a vital role in balancing the PN/A process as sufficient oxygen is required for nitritation by AerAOB, whereas excessive oxygen can further promote the nitrite oxidation to nitrate (i.e., nitratation) by nitrite-oxidizing bacteria (NOB), which should be suppressed to allow good anammox activity (Courtens et al., 2014). The difficulty of dissolved oxygen (DO) control could be a major challenge for implementing PN/A in TFs, where the air flows vertically through the filter media typically passively induced by a temperature gradient, as in a chimney. Besides the carrier porosity, the number and approaches of openings in TFs could significantly affect the DO level in the carrier biofilm by controlling the extent of passive ventilation (Bressani-Ribeiro et al., 2021; Sánchez Guillén et al., 2015). In those polyurethane (PU) sponge-TFs of Sánchez Guillén et al. (2015) and Watari et al. (2020), each sponge sheet was supported by a perforated aluminium plate, and the natural air convection was realized through lateral openings above each sponge layer (Sánchez Guillén et al., 2015; Watari et al., 2020). Even though manipulating the DO through lateral openings gives flexibility, this solution is more expensive and not easily scalable. Compared to these PU sponge-TFs, TFs based on a solid bed filled with more rigid non-compressible carriers are more straightforward in structure and installation, and thus more attractive for applications (Lekang & Kleppe, 2000). Passive ventilation openings (top only vs. top and bottom) in packed-bed TFs would be more practical, but it is unclear whether the DO can sufficiently be managed for autotrophic TN removal. The feasibility of such a simpler DO control strategy has not been tested so far.

Besides DO control, an optimal hydraulic condition is another prerequisite of a balanced PN/A process (Vlaeminck et al., 2012). It was suggested that the hydraulic loading rate (HLR) of TFs could affect carrier humidity and the amount of oxygen sucked into the reactor (Afzalimehr & Anctil, 2000; Andersson et al., 1994; EPA, 2000). The minimum HLR should ensure complete media wetting under all influent conditions, which is dependent on the media employed in the TF and typically ranges from 1 to 3 $m^3\ m^{-2}\ h^{-1}$ (EPA, 2000). In the view of good reactor performance and energy conservation, it was important to investigate the optimal HLR in different packed-bed PN/A-TFs.

Free ammonia (FA) is considered a readily available and endogenous inhibitor of NOB activity in wastewater treatment plants (WWTPs) with anaerobic digestion (Peng et al., 2020; Vlaeminck et al., 2012). In-situ low FA conditions (e.g., 0.3- 3 mg N L^{-1}) resulting from residual NH_4^+ in the PN/A reactors (e.g., SBR, RBC, and MBBR) could successfully suppress NOB activity (Kim et al., 2023; Vlaeminck et al., 2009; Zhao et al., 2022), which seems to be more labor-saving than FA shock treatment by high concentrations (e.g., 30 mg N L^{-1}), especially in long-term operations (Peng et al., 2020;

Van Tendeloo et al., 2021). Yet, the performance of in-situ low FA on NOB suppression in PN/A-TFs was barely investigated.

The overall goal of this study was to test the feasibility of PN/A in a simple and inexpensive TF design based on a packed bed and on ventilation openings at the top only and bottom. According to the information, this is the first report testing such packed-bed PN/A-TF approach. It was a sub-objective to screen for a suitable carrier material. Two conventional and commercially available plastic products were tested (polypropylene and polyethylene), next to one less costly mineral alternative (expanded clay). Furthermore, it was the ambition to determine the optimal ventilation regime (open or closed at the bottom), hydraulic loading rate, and FA level, to derive a rudimentary set of operational and design guidelines. Finally, it was a goal to understand how the activity was vertically stratified over the TFs. Synthetic autotrophic wastewater was used containing 100-250 mg NH_4^+-N L^{-1}, considered medium-strength for nitrogen (Yu et al., 2007), was fed into the TFs over a long-term experimental period (i.e., 300 days).

2. Materials and methods

2.1 Trickling filter configuration

Three lab-scale trickling filters (TFs) with the same dimensions and configuration were built for this study. Each TF was constructed from polyvinyl chloride (PVC) cylinders with a diameter of 11 cm and a height of 105 cm, consisting of three separate compartments (each 35 cm in height) (Fig. 1). The volume of each TF was 10 L. The top cap on each TF was evenly opened with 20 small holes (0.5 cm in diameter) to let the airflow draw through. A spraying apparatus was installed at the top of each TF, ensuring water was distributed homogeneously over the packed carriers. At the bottom of each TF, there was a 2 L reservoir. Water was recycled from the reservoir to the top of the TFs. There was no blockage and backflushing occurred during the whole experimental period.

Each TF was filled with a different type of carrier material: Argex crushed expanded clay aggregates (Argex, Belgium) with irregular surfaces and size as TF-A, polypropylene (PP) Bioball as TF-B, and polyethylene (PE) Kaldnes K1 as TF-K. The characteristics of the three types of carrier materials are shown in Table 1.

2.2 Influent compositions

Synthetic wastewater was used as the influent, consisting of $(NH_4)_2SO_4$, $NaHCO_3$, KH_2PO_4 (10 mg P L^{-1}), and 2 mL L^{-1} trace element solution (Kuai & Verstraete, 1998). The initial influent nitrogen concentration was approximately 100 mg NH_4^+-N L^{-1}, with a dosage of 18 mg $NaHCO_3$ mg^{-1} N. After day 158, their concentrations increased to around 250 mg NH_4^+-N L^{-1} and 24 mg $NaHCO_3$ mg^{-1} N (see supplementary material).

2.3 Trickling filter operation

A mixture of PN/A biofilm taken from a pilot-scale RBC (Meulman et al., 2010) and lab-scale RBC (Courtens et al., 2014) was used as the inoculum for all three TFs. The inoculum was recirculated in the TFs for 48 h to make the biofilm pre-attached on carriers as many as possible before the formal experiment. To simulate the warm climate in tropical countries, the TFs were operated at 30±1 °C in a temperature-controlled room. According to the flowrate parameter of pumps, the Influent was designed to be sprayed semi-continuously over the top of the TFs (1.25 min on, 8.75 min off), with a feeding flow rate of 22±2 L d^{-1}. The hydraulic loading rate (HLR) was determined by the flow rate of continuous recirculation pumps and the sectional area of the TF, expressed as 'm^3 m^{-2} h^{-1}' and shown in the top tables of Fig. 2. The recirculation ratio (i.e., the ratio of recirculation flowrate to influent flowrate) was in a range of 3.9 to 24.2 (see supplementary material).

The whole operation period was divided into nine phases (I-IX). A new phase started when a parameter was changed to improve the performance of the PN/A process. Every operational parameter change, e.g., HLR and ventilation approaches, was simultaneously applied in all three TFs. The DO in carrier biofilm was indirectly controlled by adjusting the passive ventilation openings (i.e., top, or top and bottom), HLR, or aerating in the reservoir. So-called top ventilation (phases I-II and VI-VIII) means the top cap was uncovered, but the bottom was still under the bulk solution of the reservoir. When no passive ventilation (phases III-V) was carried out, the bottom of the TF was submerged in the bulk solution, while the top was sealed entirely. In phase V, active aeration in the TF reservoir was implemented by aeration pumps to introduce DO into the recirculation flow and consequently provide DO for carrier biofilm. Once the top and bottom ventilation was implemented (phase IX), the TF was put onto a higher support structure, so that the bottom was no longer submerged in the bulk solution but exposed to the surrounding atmosphere. The passive ventilation allows the environment air to get into the TF, while adjusting HLR was expected to influence the DO level in the TF by inducing air suck and wetting the biofilm. The parallel operational conditions for all three TFs are detailed in the top table of Fig. 2 and Fig.3.

The pH was measured daily by a portable, digital pH meter C833 (Consort, Belgium). The DO concentration in the reservoir was measured daily by a portable digital oxygen meter HQ30d (Hach Lange, Germany). The influent and effluent samples were taken periodically from the influent vessel and the reservoir, respectively. The samples were immediately filtered with 0.45 μm filters and stored at 4 °C until the analysis of NH_4^+-N, NO_2^--N, and NO_3^--N concentrations.

2.4 Determination of microbial activity in each compartment

Microbial activity in three compartments of each TF was determined on day 259 (phase IX) via three rounds of batch tests. Before each round of the tests, the recirculation pump was turned off, then the columns were left to stand for 30 mins to drain the water out. The reservoir at the bottom of each TF was then filled with 2 L of tap water containing 100 mg NH_4^+-N L^{-1} and 24 mg $NaHCO_3$ mg^{-1} N as a buffer to keep the pH at around 7.5. The recirculation pump was then turned on again with the same HLR as in phase IX (i.e., 1.8 m^3 m^{-2} h^{-1}). The first-round batch test was carried out for the whole TF. In the second round, the bottom compartment was taken down, and the two upper compartments were kept for the activity test. Finally, the third-round batch test was performed only in the top compartment. The batch test in every round lasted for 180 mins and samples were taken from the reservoir every 30 mins.

2.5 Physicochemical water analyses and microbial activity calculations

NH_4^+-N was determined according to the standard Nessler method (Greenberg et al., 1992). NO_2^--N and NO_3^--N were determined on a 761 compact ion chromatograph equipped with a conductivity detector (Metrohm, Switzerland). FA levels in TFs were calculated based on the reactor ammonium concentration, pH, and temperature (Anthonisen et al., 1976).

The microbial activity of the AerAOB, AnAOB, and NOB in the TFs was calculated based on the anammox stoichiometry (Strous et al., 1998) and mass balance of the nitrogen compounds according to Eq. (2), (3), and (4) (Strous et al., 1998; Vlaeminck et al., 2012). Heterotrophic denitrification was assumed to be neglectable due to the autotrophic influent. The AerAOB activity was determined as the sum of

NO_2^--N consumption by the NOB and AnAOB, and residual NO_2^--N production ($P_{NO_2^--N}$). The AnAOB activity was determined by the TN removal (R_{TN}, i.e., complete conversion to N_2) and the 11% NO_3^--N production by AnAOB (Eq. (1)). The NOB activity was calculated based on the total NO_3^--N production ($P_{NO_3^--N}$) subtracted by the NO_3^--N production by AnAOB.

$$\text{AerAOB activity (mg N L}^{-1}\text{ d}^{-1}) = (P_{NO_2^--N}) + (P_{NO_3^--N} - \frac{0.11}{0.89} * R_{TN}) + (\frac{1.32}{2.32} * (R_{TN} + \frac{0.11}{0.89} * R_{TN})) \quad (2)$$

$$\text{AnAOB activity (mg N L}^{-1}\text{ d}^{-1}) = R_{TN} + \frac{0.11}{0.89} * R_{TN} \quad (3)$$

$$\text{NOB activity (mg N L}^{-1}\text{ d}^{-1}) = P_{NO_3^--N} - \frac{0.11}{0.89} * R_{TN} \quad (4)$$

3. Results and discussion

The PN/A performance of TF-A is elaborately shown in Fig. 2. Since the overall performance trends in TF-B and TF-K are similar to TF-A (see supplementary material), only the key results of these two reactors were highlighted in Fig. 3 and discussed in this section.

3.1 Start-up periods: nitrate accumulation

Phase I and II are considered the start-up periods, when ventilation was allowed only from the top of the TFs. The bulk solution was recirculated continuously with an HLR of 0.8 m^3 m^{-2} h^{-1} in phase I. The NH_4^+-N removal efficiencies were around 54% in all three TFs (e.g., Fig. 2b), while the TN removal efficiency was much lower (averaged below 20%), mainly due to the high NO_3^--N production (relative to the NH_4^+-N removal corrected by the NO_2^--N accumulation) of 71±6%, 54±3%, and 64±15% in TF-A, TF-B, and TF-K, respectively. The NO_2^--N accumulation of around 60% (relative to the removed NH_4^+-N) was initially observed in all three TFs, indicating that

NOB and AnAOB were both limited initially. Over time, NO_2^--N accumulation gradually decreased in phase I, and NOB won the competition for NO_2^--N over anammox due to the relatively high DO (0.6-1.1 mg O_2 L^{-1}, the top tables of Fig.2 and Fig. 3). In phase II of TF-A, under a lower HLR of 0.4 m^3 m^{-2} h^{-1}, the NO_3^--N production efficiency decreased to 30±2%. Combined with the further increase of NH_4^+-N removal and decrease of NO_2^--N accumulation, the TN removal efficiency increased to 51±3%. By the end of phase II, the TN removal rates stabilized at 132±12 N L^{-1} d^{-1} (Fig. 2c).

For passive aeration, oxygen in the air is firstly transported to the liquid phase, then diffused into the biofilm, and eventually consumed by aerobic bacteria, such as AerAOB and NOB. The improved TN removal performance from phase I to II could be related to the change in the activity of functional bacteria (i.e., AerAOB, AnAOB, and NOB, Fig. 2d) in carrier biofilm. Thus, the activity changes could be attributed to the decreased DO concentration in the reactors induced by the lowered HLR in phase II, as decreasing the HLR may induce less oxygen being sucked into the reactor (Afzalimehr & Anctil, 2000; Andersson et al., 1994). AerAOB often have a higher oxygen affinity than NOB, with the typical half-saturation constant K_s of 0.6 and 2.2 mg O_2 L^{-1}, respectively (Hao et al., 2002). Thus, at low DO concentrations (< 1 mg O_2 L^{-1}), AerAOB would more preferentially metabolize the DO, limiting the NOB activity (Van Tendeloo et al., 2021). Another possible explanation could be the increased biofilm thickness over time, which created more anoxic zones that promoted and protected the AnAOB activity (Pynaert et al., 2003; Vlaeminck et al., 2010).

3.2 Effect of top passive ventilation

To further decrease the NO_3^--N production via lowering the DO concentration in the TFs, both the top and bottom ventilation were stopped in phase III. The NO_3^--N production significantly decreased to 12±4%, 25±5%, and 25±1% in TF-A, TF-B, and

TF-K, respectively (Fig. 2b and Fig. 3). No NO_2^--N accumulation was observed in any TF. However, stopping the top ventilation caused the decrease of NH_4^+-N removal efficiency to around 24% in all three TFs, probably attributed to the insufficient oxygen for AerAOB. Compared to phase II, the lower DO level in the reservoirs implied the DO scarcity in the TFs (top tables of Fig.2 and 3). The sharply decreased NH_4^+-N removal negated the desired decrease of NO_3^--N production, causing the TN removal efficiency to drop to around 20% in all TFs (Fig. 2b and Fig. 3).

In phase IV, the HLR was recovered to 0.8 m^3 m^{-2} h^{-1}, aiming to raise the DO level and the consequent NH_4^+-N oxidation efficiency in the TFs. However, only increasing the HLR failed to achieve these goals (e.g., Fig. 2). Since the TFs were completely closed, no air could be sucked in, and the sole DO source was the oxygen dissolved into the bulk solution. In phase V, aeration pumps were installed in the reservoir to actively introduce more DO into the recirculation stream. The active aeration successfully promoted the NH_4^+-N oxidation in all three TFs, particularly in TF-A (from 11±2% to 50±7%), indicating the low DO concentration was a limiting factor.

In phase VI, the top passive ventilation replaced the active aeration in the reservoir. Meanwhile, the influent concentration was increased to about 250 mg NH_4^+-N L^{-1}. The average concentrations of effluent NH_4^--N and NO_3^--N were visibly increased after day 158, due to the increased influent TN loading rate (Fig. 2a and 2c). Meanwhile, the NH_4^+-N removal efficiency increased to around 60% in all three TFs. Compared to phase I with the same HLR, phase VI got a similar NH_4^+-N conversion efficiency but a lower NO_3^--N production efficiency of around 32% (Fig. 2b and 3). As a result, the TN removal efficiency increased to approximately 42% in all three TFs. Furthermore, due to increasing the influent loading rate, the TN removal rate increased to about 184 mg N L^{-1} d^{-1} for all three TFs (Fig. 2c and Fig. 3).

The highest NO_3^--N production observed during the start-up periods indicated the most robust NOB activity in carrier biofilm. When the top passive ventilation was forbidden, NO_3^--N production and NH_4^+-N removal dropped drastically as a limited amount of DO was introduced into the TFs. Thus, passive ventilation (e.g., from the top, phase VI) was necessary to get enough oxygen into the TFs for the partial nitritation process. Meanwhile, an increase in pH from around 7.0 to 7.5 was observed due to the lowered protons (H^+) production via nitritation and nitratation processes. With the rise of the residual NH_4^+-N and pH, the free ammonia (FA) level in all three TFs increased from around 0.3 mg N L^{-1} to above 1.3 mg N L^{-1} in phases III and IV (e.g., Fig. 2a). NOB were suggested to be more sensitive to FA (> 0.08- 0.82 mg N L^{-1}) than that of AerAOB (> 8-120 mg N L^{-1}) treatment (Vlaeminck et al., 2012). Zhao et al. (2022) reported long-term NOB suppression in PN/A biofilms at residual ammonium concentration of 50 mg N L^{-1} (pH 7.2, 22°C), equivalent to FA of 0.36 mg N L^{-1} (Zhao et al., 2022). In a single-stage deammonification SBR system, FA higher than 1.0 mg/L contributed to suppressing NOB activity (Kim et al., 2023), while in a PN/A-RBC system, controlling the FA level at 3 mg N L^{-1} was considered a good NOB inhibition strategy (Vlaeminck et al., 2009). The bulk FA circumstance herein probably improved the NOB suppression and partially contributed to the almost vanished NOB activity in phase III and IV (e.g., Fig. 2d). Based on a previous study, including the AnAOB biofilm in such FA level could not only be mostly harmless to the AnAOB community, but also avoid migration of NOB activity towards the biofilm (Peng et al., 2020). Besides, it should be noted that NOB could get acclimated to high FA levels in long term, and that DO control at a relatively low set point (e.g., 0.2-0.5 mg O_2 L^{-1}) could also be essential (Kim et al., 2023; Vlaeminck et al., 2009; Zhao et al., 2022).

3.3 Effect of hydraulic loading rate

In phases VII and VIII, the effect of HLR was investigated under the top passive ventilation situation. The HLR was increased to 1.8 and 2.2 m^3 m^{-2} h^{-1} in phases VII and VIII, respectively. In phase VII, the NH_4^+-N conversion efficiency further increased, while the NO_3^--N production kept decreasing, especially in TF-A, to 64±8% and 13±1%, respectively. Hence, the TN removal efficiency increased to 52±7%, 59±4%, and 55±3%, and the TN removal rate reached 269±34, 300±23, and 251±19 mg N L^{-1} d^{-1} in TF-A, TF-B, and TF-K, respectively (Fig. 2c and 3). In phase VIII, after increasing the HLR to 2.2 m^3 m^{-2} h^{-1}, no further improvement of the NH_4^+-N conversion and TN removal efficiency was observed. Since higher HLR means more electrical energy consumption by recirculation pumps, the optimal HLR was considered to be 1.8 m^3 m^{-2} h^{-1}. Normally, a fraction of the free-draining volume is trapped within the carrier biofilm and does not circulate under normal feed conditions (Séguret et al., 2000). In this case, TFs as attached growth systems can withstand longer starvation periods without losing significant biomass (Cramer et al., 2021). Hence, although the wetting extent of the carrier biofilm could not be guaranteed when the HLR was relatively small (0.4-0.8 m^3 m^{-2} h^{-1}), the immobile biomass probably remained to be starving rather than dying. The typical HLR in TFs was suggested between 1 to 3 m^3 m^{-2} h^{-1} to keep carrier material moist (EPA, 2000), which was roughly consistent with that of the PU sponge TFs (1.3-3.3 m^3 m^{-2} h^{-1}) (Sánchez Guillén et al., 2015). The optimal HLR found in this study, i.e., 1.8 m^3 m^{-2} h^{-1}, was within this recommended range as well. Thus, the higher TN removal efficiency at 1.8 m^3 m^{-2} h^{-1} could be partly attributed to the more completely wetted biofilm. Additionally, the relatively high FA level in phase VII (3.2±0.7 mg N L^{-1} of TF-A, Fig. 2a) also improved PN/A performance by inhibiting NOB activity. There were no signs of NOB adaptation observed for the FA treatments under the relatively low DO circumstance in the long term. Both the FA inhibition and low DO are needed to suppress nitration process, which was consistent with previous studies (Kent et al., 2019; Van Tendeloo et al., 2021; Vlaeminck et al., 2009).

3.4 Effect of ventilation from the bottom

In phase IX, the bottom of the TFs was lifted out of the bulk solution in reservoirs, enabling passive ventilation via both the top and bottom of the TFs. The reservoir DO raise in TF-A (0.3±0.1 to 0.4±0.2 mg O_2 L^{-1}) was less than that of TF-B (0.5±0.1 to 0.9±0.2 mg O_2 L^{-1}) and TF-K (0.3±0.2 to 1.0±0.3 mg O_2 L^{-1}), probably related to the porosity of the carrier materials (Table 1). The higher porosity of Argex in TF-A probably introduced more vertical airflow through the filter media by air draft via only the top ventilation, consequently allowing more oxygen to reach the bottom compartment. Thus, further allowing the bottom ventilation had a lower impact in TF-A than that in the other two TFs. This hypothesis was consistent with the relatively stable NH_4^+-N and NO_3^--N conversion performance in TF-A before (58± 8 % and 16± 6 %) and after (59± 9 % and 18± 4 %) allowing bottom ventilation, respectively (Fig. 2). The decreased FA level from 1.6±0.3 mg N L^{-1} (phase VII) to 0.7±0.3 mg N L^{-1} (phase IX) in TF-K (see supplementary material) may explain the increased NO_3^--N production efficiency in TF-K.

The nitrogen removal rates in this study were relatively moderate (around 300 mg N L^{-1} d^{-1}) compared to other PN/A biofilm reactors (35- 874 mg N L^{-1} d^{-1}) (Bressani-Ribeiro et al., 2021; Sánchez Guillén et al., 2015; Van Tendeloo et al., 2021; Watari et al., 2020). Although the TFs failed to realize higher nitrogen removal efficiency like those active-aerating PN/A systems (> 80%), their relatively high nitrogen loading rates (> 500 mg N L^{-1} d^{-1}) and short HRT (i.e., 0.1 days) could be more suitable for the post-treatment of anaerobic sewage in the domestic WWTPs of tropical countries, focusing more on the ammonium removal rather than TN removal (Arthur et al., 2022; Bressani-Ribeiro et al., 2018).

Overall, controlling the DO level in the TFs was difficult as it was measured in the reservoir, which was a combined result of the oxygen dissolved into the reservoir, ventilated into TFs, and consumed by aerobic bacteria (e.g., AerAOB and NOB). Nevertheless, the TN removal performance via the combined passive ventilation in phase IX was comparable to that in phase VII for all three TFs (Fig. 2 and 3). Therefore, it could be concluded that additional passive ventilation from the top and bottom ventilation could not further facilitate TN removal and was unnecessary.

3.5 Vertical stratification of activity in trickling filters

The TFs used in this study consisted of three vertical compartments (top, middle, and bottom). Batch tests were carried out on day 259 (phase IX, top and bottom ventilation) to quantify the microbial activity of AerAOB, AnAOB, and NOB in each compartment (Eq. 2-4, section 2.5). In TF-A, the AerAOB activity increased from the top (290 mg N L^{-1} d^{-1}) to the bottom compartment (461 mg N L^{-1} d^{-1}) (Fig. 4). The highest AnAOB activity in the top compartment accounted for about 65% of the total AnAOB activity. The NOB activity increased from the top to the bottom, with 46% activity in the bottom compartment. In TF-B, the AnAOB activity was highest in the top compartment (403 mg N L^{-1} d^{-1}), but almost zero in the bottom compartment. The NOB activity was low and approximately equal in all compartments (45±9 mg N L^{-1} d^{-1}). Similar to TF-A, the highest AnAOB activity was in the top compartment of TF-K, while the highest NOB activity was found in the bottom, accounting for 46%.

The measured microbial activity in the different compartments of the TFs depended on the suitability of microenvironments (e.g., substrate availability) for the specific microorganisms before the activity tests. It has been shown in Section 3.4 that bottom ventilation has less effect on improving TN removal efficiencies, and the introduced DO mainly depended on top ventilation and recirculation. Therefore, the DO at the upper layer should be the highest, which benefits the growth of AerAOB and subsequently the generation of NO_2^--N. Meanwhile, the continuous oxygen demand by AerAOB could protect AnAOB in the deeper biofilm layers from oxygen penetration and inhibition (Van Tendeloo et al., 2021). The ammonium-rich influent was sprayed over the top of the TFs, resulting in the highest NH_4^+-N level in the top compartment. Therefore, both the biofilm structure and the availability of nitrogen substrates (i.e., NH_4^+-N and NO_2^--N) in the top compartment make the AnAOB activity the highest among the three compartments for all the tested TFs. In addition, substrate competition (e.g., DO, NH_4^+-N, and NO_2^--N) among those bacteria also contributes to the vertical stratification of community activity in TFs. In TF-A, the increasing AerAOB activity from top to bottom could be the combined effects of the DO and AnAOB competition. Similarly, the lower competition for NO_2^--N from AnAOB in the bottom compartment may allow the proliferation of NOB activity (Fig. 4). In TF-B, it was striking that the microbial activity in the bottom compartment was much lower than in the other TFs (Fig. 4). It was likely due to the biomass loss by water washout. The low specific surface area of TF-B (Table 1) was suggested to grow ticker biofilm (Hu et al., 2020), which is much less stable and easier to be removed by the water flow (Melo & Vieira, 1999). In TF-K, the AerAOB and NOB activity decreased in the middle compartment but increased again in the bottom compartment (Fig. 4). The increased AerAOB and NOB activity in the bottom compartment might benefit from the bottom ventilation, which may lead to the DO increase there.

3.6 Carrier material and electrical energy consumption

For all three types of TFs, the highest TN removal efficiency of 60% and TN removal rate of 300 mg N L^{-1} d^{-1} were achieved in phase VII, with only top ventilation and optimal HLR (1.8 m^3 m^{-2} h^{-1}) (Fig. 2 and 3). Notably, a relatively low NO_3^--N production of 13% was achieved for the first time via the PN/A process implemented in a TF. In the three PU sponge-TF studies, the TN removal efficiency and NO_3^--N production efficiency ranged from 26% to 54% and 25% to 61%, respectively (Bressani-Ribeiro et al., 2021; Sánchez Guillén et al., 2015; Watari et al., 2020). Thus, higher TN removal efficiency and lower NO_3^--N production efficiency were achieved in this study. Since the TN removal performance with the three types of carriers was similar, the lowest price of only 42 € m^{-3} makes Argex economically attractive to apply PN/A technology in a TF (Table 1).

In the designed TFs, oxygen is passively introduced into the columns. Instead of the energy-consuming aeration pump, a recirculation pump becomes the energy-consuming item. To calculate its electrical energy consumption, several parameters were assumed, including a daily nitrogen production per capita (person) of 3.7 g N d^{-1} (Cheng et al., 2021), reactor height of 105 cm, pump depth in the reservoir of 20 cm, a pipe head loss of 0.33 m m^{-1} pipe and a high pump efficiency of 80% (Spellman, 2013). The calculated electrical energy consumption was 0.78 kWh kg^{-1} N removal under the TN removal rate of 300 mg N L^{-1} d^{-1} (phase VII), which was 1.9 times higher than an RBC (0.4 kWh kg^{-1} N) (Mathure & Patwardhan, 2005), but 35% more energy-efficient than an actively aerated SBR (1.2 kWh kg^{-1} N) (Wett et al., 2010).

Although the packed-bed PN/A-TFs show economical, practical, and scalable superiorities in improving the effluent quality of anaerobic sewage treatment in tropical areas, they still have a huge progress to be made in increasing TN removal efficiency.

Currently, only around 60% of TN removal efficiency was achieved under the optimal HLR of 1.8 m^3 m^{-2} h^{-1}. In fact, further improving the TN removal efficiency would raise the effluent quality and make the packed-bed PN/A-TFs much more energy-efficient. Decreasing the influent NH_4^+-N loading rate (e.g., to two third of phase VII by lowering the influent flow rate) may facilitate the increase of TN removal rates as the TF operation in this study was influent NH_4^+-N overload. Besides, slightly prolonging the time interval of batch feedings would contribute to cyclically returning the high FA (e.g., 3.2 mg N L^{-1}) but still low TAN towards the end of the batch operation. Both these two strategies are easy to be implemented without dosing additional chemicals (e.g., carbon sources). Especially for the latter strategy, maintaining sufficiently high FA levels in recirculation flow could contribute to the low nitrate production rate due to the effective NOB suppression. Anyway, further optimization strategies may be required to improve the TN removal efficiency while maintaining sufficiently high FA levels for NOB suppression.

Nevertheless, the feasibility of packed-bed PN/A-TFs that were filled with rigid incompressible carriers was proved for the first time. The TF-A using expanded clay as inexpensive mineral carriers was recommended due to their economical efficiency. The hydraulic loading rate, passive ventilation regime, and in-situ FA level were suggested as three key parameters in maintaining a successful PN/A-TF system. A rudimentary set of operational and design guidelines proposed here are valuable for warm climate regions to apply packed-bed PN/A-TFs as a cost-effective nitrogen removal approach.

4. Conclusions

This study demonstrated the feasibility of packed-bed PN/A-TFs, and hence very energy-efficient TN removal. The tests showed that passive ventilation at the top is sufficient to supply oxygen for PN/A. For all three TFs, more than 56% of AnAOB activity was found in the top compartment. Under an optimal HLR of 1.8 $m^3 m^{-2} h^{-1}$, the TN removal rate reached 300 mg N $L^{-1} d^{-1}$ (30 °C). FA of 1.3-3.2 mg N L^{-1} likely contributed to NOB suppression. Moreover, the inexpensive carrier based on expanded clay can be recommended due to the similar TN removal rates as commercially used plastics.

Supplementary material

E-supplementary data for this work can be found in e-version of this paper online.

Acknowledgments

The authors would like to acknowledge the financial support for Siegfried E. Vlaeminck through a postdoctoral fellowship from the Research Foundation - Flanders (FWO) and for Yankai Xie from the China Scholarship Council (File no. CSC201706130131).

References

1. Afzalimehr, H., Anctil, F. 2000. Accelerating shear velocity in gravel-bed channels. *Hydrological Sciences Journal*, 45(1), 113-124.
2. Andersson, B., Aspegren, H., Parker, D., Lutz, M. 1994. High rate nitrifying trickling filters. *Water science and technology*, 29(10-11), 47.
3. Anthonisen, A., Loehr, R., Prakasam, T., Srinath, E. 1976. Inhibition of nitrification by ammonia and nitrous acid. *Journal (Water Pollution Control Federation)*, 835-852.
4. Arthur, P.M.A., Konaté, Y., Sawadogo, B., Sagoe, G., Dwumfour-Asare, B., Ahmed, I., Williams, M.N.V. 2022. Performance evaluation of a full-scale upflow anaerobic sludge blanket reactor coupled with trickling filters for municipal wastewater treatment in a developing country. *Heliyon*, 8(8), e10129.
5. Bressani-Ribeiro, T., Almeida, P., Volcke, E., Chernicharo, C. 2018. Trickling filters following anaerobic sewage treatment: state of the art and perspectives. *Environmental Science: Water Research & Technology*, 4(11), 1721-1738.
6. Bressani-Ribeiro, T., Almeida, P.G.S., Chernicharo, C.A.L., Volcke, E.I.P.

2021. Inorganic carbon limitation during nitrogen conversions in sponge-bed trickling filters for mainstream treatment of anaerobic effluent. *Water Research*, 117337.
7. Cheng, F., Dai, Z., Shen, S., Wang, S., Lu, X. 2021. Characteristics of rural domestic wastewater with source separation. *Water Science and Technology*, 83(1), 233-246.
8. Courtens, E.N.P., Boon, N., De Clippeleir, H., Berckmoes, K., Mosquera, M., Seuntjens, D., Vlaeminck, S.E. 2014. Control of nitratation in an oxygen-limited autotrophic nitrification/denitrification rotating biological contactor through disc immersion level variation. *Bioresource Technology*, 155, 182-188.
9. Cramer, M., Tränckner, J., Kotzbauer, U. 2021. Kinetic of denitrification and enhanced biological phosphorous removal (EBPR) of a trickling filter operated in a sequence-batch-reactor-mode (SBR-TF). *Environmental Technology*, 42(17), 2631-2640.
10. De Clippeleir, H., Vlaeminck, S.E., De Wilde, F., Daeninck, K., Mosquera, M., Boeckx, P., Verstraete, W., Boon, N. 2013. One-stage partial nitritation/anammox at 15 °C on pretreated sewage: feasibility demonstration at lab-scale. *Applied Microbiology and Biotechnology*, 97(23), 10199-10210.
11. De Clippeleir, H., Yan, X., Verstraete, W., Vlaeminck, S.E. 2011. OLAND is feasible to treat sewage-like nitrogen concentrations at low hydraulic residence times. *Applied Microbiology and Biotechnology*, 90(4), 1537-1545.
12. EPA, E.P.A. 2000. Wastewater technology fact sheet: Trickling filter nitrification.
13. Greenberg, A., Clesceri, L., Eaton, A. 1992. Standard methods for the examination of water and wastewater. Published by American public health association 18th edition Washington, DC. *Library congress ISBN 0-87553-207-1*.
14. Hao, X., Heijnen, J.J., Van Loosdrecht, M.C.M. 2002. Sensitivity analysis of a biofilm model describing a one-stage completely autotrophic nitrogen removal (CANON) process. *Biotechnology and Bioengineering*, 77(3), 266-277.
15. Hu, X., Lin, R., Wei, J., Chang, J., Wang, K., Zhong, M., Chen, L. 2020. Effects of Internal Diameter Size of Carriers on Biofilm Characteristics in Wastewater Treatment. *Environmental Engineering Science*, 37(10), 679-688.
16. Kent, T.R., Sun, Y., An, Z., Bott, C.B., Wang, Z.-W. 2019. Mechanistic understanding of the NOB suppression by free ammonia inhibition in continuous flow aerobic granulation bioreactors. *Environment International*, 131, 105005.
17. Kim, J., Direstiyani, L.C., Jeong, S., Kim, Y., Park, S., Yu, J., Lee, T. 2023. Feeding strategy for single-stage deammonification to treat moderate-strength ammonium under low free ammonia conditions.

Science of The Total Environment, 857, 159661.

18. Kuai, L., Verstraete, W. 1998. Ammonium Removal by the Oxygen-Limited Autotrophic Nitrification-Denitrification System. *Applied and Environmental Microbiology*, 64(11), 4500-4506.
19. Lekang, O.-I., Kleppe, H. 2000. Efficiency of nitrification in trickling filters using different filter media. *Aquacultural engineering*, 21(3), 181-199.
20. Lombard-Latune, R., Pelus, L., Fina, N., L'Etang, F., Le Guennec, B., Molle, P. 2018. Resilience and reliability of compact vertical-flow treatment wetlands designed for tropical climates. *Science of The Total Environment*, 642, 208-215.
21. Mathure, P., Patwardhan, A. 2005. Comparison of mass transfer efficiency in horizontal rotating packed beds and rotating biological contactors. 80(4), 413-419.
22. Melo, L.F., Vieira, M.J. 1999. Physical stability and biological activity of biofilms under turbulent flow and low substrate concentration. *Bioprocess Engineering*, 20(4), 363.
23. Meulman, B., Elzinga, N., Gorter, K., Zeeman, G., Buisman, C., Vlaeminck, S., Verstraete, W. 2010. Pilot-scale demonstration of sustainable C and N removal from concentrated black water. *IWA World Water Congress & Exhibition*.
24. Mulder, A. 2003. The quest for sustainable nitrogen removal technologies. *Water Science and Technology*, 48(1), 67-75.
25. Peng, L., Xie, Y., Van Beeck, W., Zhu, W., Van Tendeloo, M., Tytgat, T., Lebeer, S., Vlaeminck, S.E. 2020. Return-Sludge Treatment with Endogenous Free Nitrous Acid Limits Nitrate Production and N2O Emission for Mainstream Partial Nitritation/Anammox. *Environmental Science & Technology*, 54(9), 5822-5831.
26. Pynaert, K., Smets, B.F., Wyffels, S., Beheydt, D., Siciliano, S.D., Verstraete, W. 2003. Characterization of an autotrophic nitrogen-removing biofilm from a highly loaded lab-scale rotating biological contactor. *Applied and environmental microbiology*, 69(6), 3626-3635.
27. Sánchez Guillén, J.A., Jayawardana, L.K.M.C.B., Lopez Vazquez, C.M., De Oliveira Cruz, L.M., Brdjanovic, D., Van Lier, J.B. 2015. Autotrophic nitrogen removal over nitrite in a sponge-bed trickling filter. *Bioresource Technology*, 187, 314-325.
28. Séguret, F., Racault, Y., Sardin, M. 2000. Hydrodynamic behaviour of full scale trickling filters. *Water Research*, 34(5), 1551-1558.
29. Spellman, F.R. 2013. *Handbook of water and wastewater treatment plant operations*. CRC press.
30. Strous, M., Heijnen, J.J., Kuenen, J.G., Jetten, M.S.M. 1998. The sequencing batch reactor as a powerful tool for the study of slowly growing anaerobic ammonium-oxidizing microorganisms. *Applied Microbiology and Biotechnology*, 50(5), 589-596.
31. The Water Environment, F. 2011. *Biofilm Reactors - WEF MoP 35*. McGraw-Hill Education, New York.

32. Van Tendeloo, M., Xie, Y., Van Beeck, W., Zhu, W., Lebeer, S., Vlaeminck, S.E. 2021. Oxygen control and stressor treatments for complete and long-term suppression of nitrite-oxidizing bacteria in biofilm-based partial nitritation/anammox. *Bioresource Technology*, 125996.
33. Vlaeminck, S., De Clippeleir, H., Verstraete, W. 2012. Microbial resource management of one - stage partial nitritation/anammox. *Microbial Biotechnology*, 5(3), 433-448.
34. Vlaeminck, S.E., Terada, A., Smets, B.F., De Clippeleir, H.E., Schaubroeck, T., Bolca, S., Demeestere, L., Mast, J., Boon, N., Carballa, M., Verstraete, W. 2010. Aggregate Size and Architecture Determine Microbial Activity Balance for One-Stage Partial Nitritation and Anammox. *Applied and Environmental Microbiology*, 76(3), 900-909.
35. Vlaeminck, S.E., Terada, A., Smets, B.F., Linden, D.V.D., Boon, N., Verstraete, W., Carballa, M. 2009. Nitrogen Removal from Digested Black Water by One-Stage Partial Nitritation and Anammox. *Environmental Science & Technology*, 43(13), 5035-5041.
36. Watari, T., Vazquez, C.L., Hatamoto, M., Yamaguchi, T., Van Lier, J.B. 2020. Development of a single-stage mainstream anammox process using a sponge-bed trickling filter. *Environmental Technology*, 1-12.
37. Wett, B., Nyhuis, G., Takács, I., Murthy, S. 2010. Development of enhanced deammonification selector. *WATER ENVIRONMENT FEDERATION, WEFTEC*, 2-6.
38. Yu, H.-B., Quan, X., Ding, Y.-Z. 2007. Medium-strength ammonium removal using a two-stage moving bed biofilm reactor system. *Environmental engineering science*, 24(5), 595-601.
39. Zekker, I., Mandel, A., Rikmann, E., Jaagura, M., Salmar, S., Ghangrekar, M.M., Tenno, T. 2021a. Ameliorating effect of nitrate on nitrite inhibition for denitrifying P-accumulating organisms. *Science of The Total Environment*, 797, 149133.
40. Zekker, I., Raudkivi, M., Artemchuk, O., Rikmann, E., Priks, H., Jaagura, M., Tenno, T. 2021b. Mainstream-sidestream wastewater switching promotes anammox nitrogen removal rate in organic-rich, low-temperature streams. *Environmental Technology*, 42(19), 3073-3082.
41 Zhao, J., Liu, T., Meng, J., Hu, Z., Lu, X., Hu, S., Yuan, Z., Zheng, M. 2022. Ammonium concentration determines oxygen penetration depth to impact the suppression of nitrite-oxidizing bacteria inside partial nitritation and anammox biofilms. *Chemical Engineering Journal*, 140738.

Table 1. Characteristics of the carrier materials used in the TFs.

Carrier material	Argex (TF-A)	Bioball (TF-B)	Kaldnes (TF-K)
Type of material	Expanded clay	Polypropylene	Polyethylene
Diameter (mm)	4-8	42	9
Specific surface area ($m^2\ m^{-3}$)	500-1000	340	800
Porosity (%)	88	78	84
Cost (€ m^{-3}, indicative)	42	1983	1590

Figure captions

Figure 1. Schematic diagram of a packed-bed TF system.

Figure 2. Performance overview of TF-A in phase I-IX (day 0-300): (a) effluent concentration and FA level, (b) nitrogen conversion efficiency, (c) volumetric loading and conversion rates, and (d) relative activity of AerAOB, AnAOB, and NOB. The main variables per phase are shown in the top table. "N.A." represents passive ventilation was not arranged.

Figure 3. Performance overview of (a) TF-B and (b) TF-K in phase I-IX (day 0-300), including TN removal efficiency, NO_3^--N production efficiency, and TN removal rate.

Figure 4. The microbial activity of AerAOB, AnAOB, and NOB in each compartment of the TFs on day 259 in phase IX.

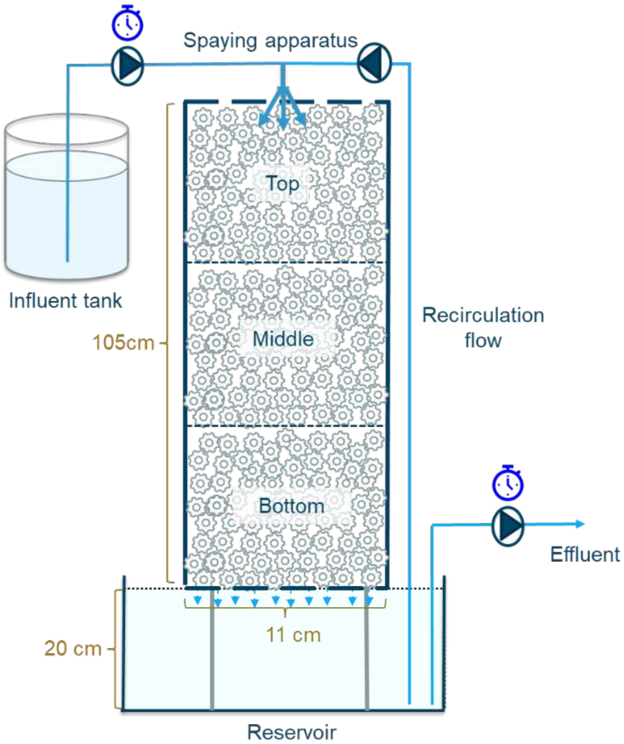

Figure 1. Schematic diagram of a packed-bed TF system.

Phase	I	II	III	IV	V	VI	VII	VIII	IX
HLR (m³ m⁻² h⁻¹)	0.8	0.4			0.8		1.8	2.2	1.8
Passive ventilation (top/bottom)	top		N.A			top			top & bottom
DO in reservoir (mg O_2 L⁻¹)	0.6±0.2	0.5±0.1	0.4±0.1		1.6±0.6	0.3±0.1			0.4±0.2

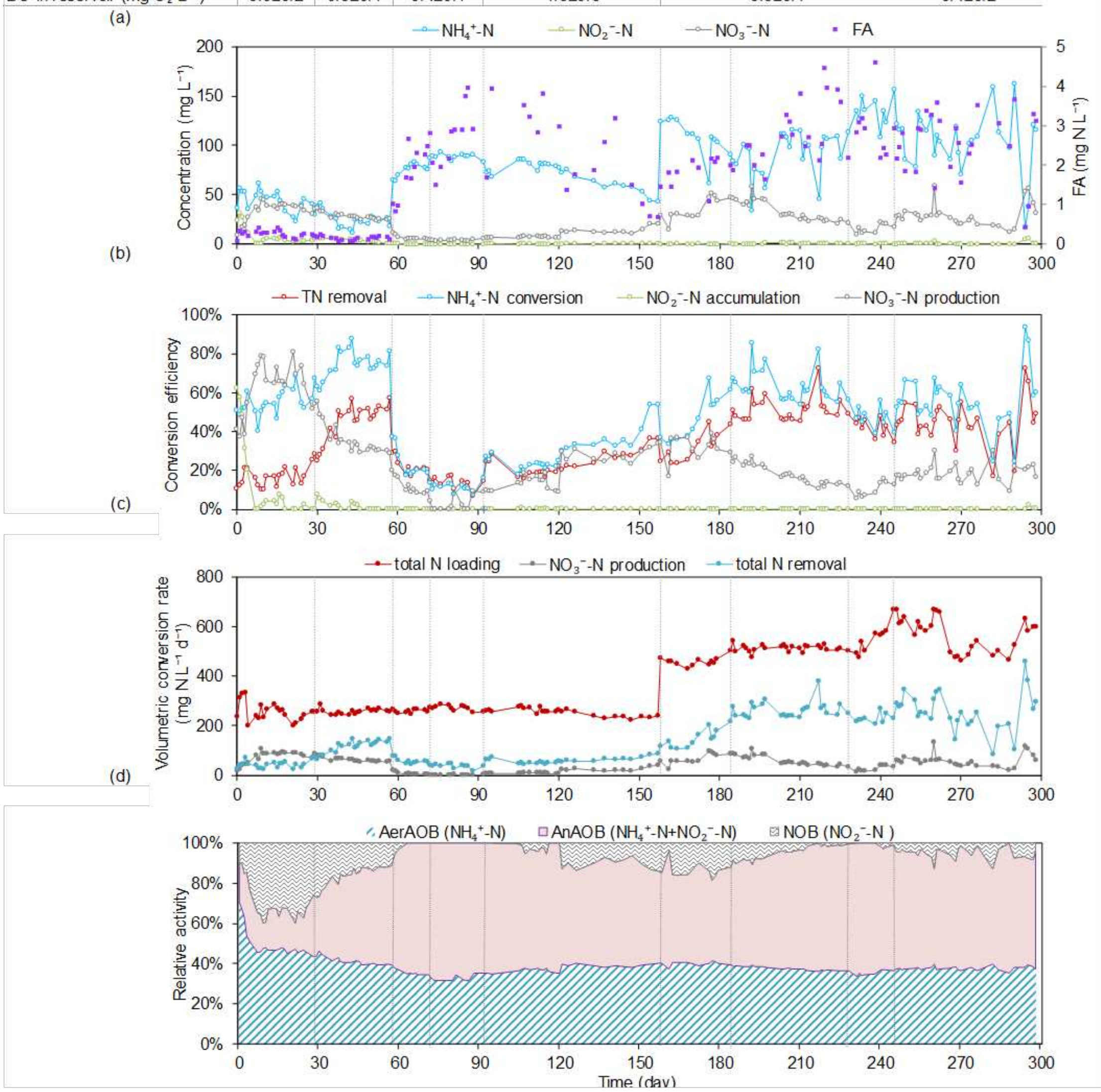

Figure 2. Performance overview of TF-A in phase I-IX (day 0-300): (a) effluent concentration and FA level, (b) nitrogen conversion efficiency, (c) volumetric loading and conversion rates, and (d) relative activity of AerAOB, AnAOB, and NOB. The main variables per phase are shown in the top table. "N.A." represents passive ventilation was not arranged.

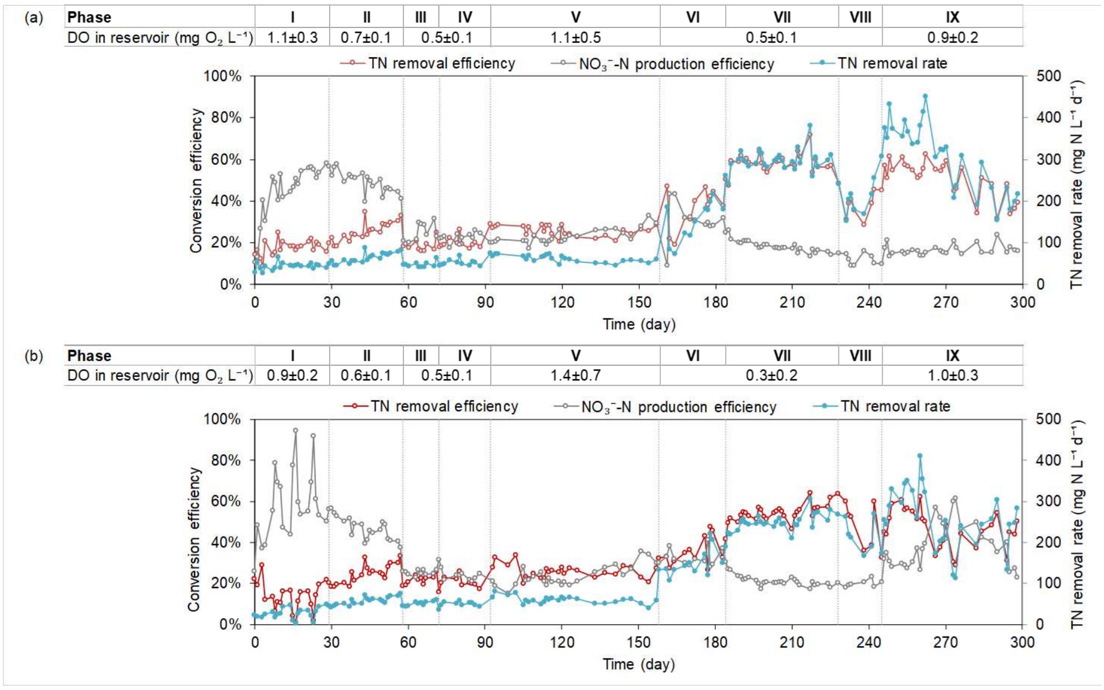

Figure 3. Performance overview of (a) TF-B and (b) TF-K in phase I-IX (day 0-300), including TN removal efficiency, NO_3^--N production efficiency, and TN removal rate.

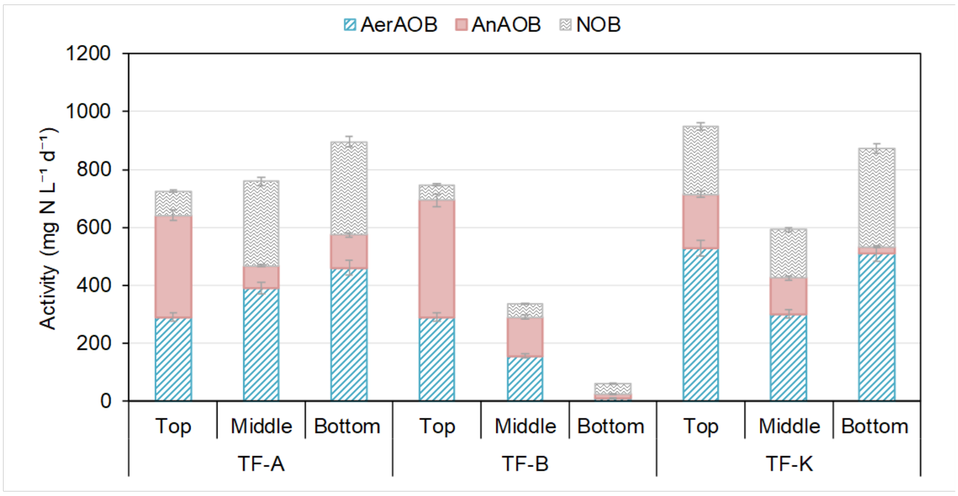

Figure 4. The microbial activity of AerAOB, AnAOB, and NOB in each compartment of the TFs on day 259 in phase IX.